1992

# Efficiency Improvement of Inverter Rotary Compressor by the Optimal Design of Vane

J. Park
*Samsung Electronics Company; Korea*

W. Lee
*Samsung Electronics Company; Korea*

H. Kim
*Samsung Electronics Company; Korea*

# EFFICIENCY IMPROVEMENT OF INVERTER ROTARY COMPRESSOR BY THE OPTIMAL DESIGN OF VANE

Jeongsoo Park [1], Wonseok Lee[2], Hyungsuk Kim[2]
R&D CENTER, SAMSUNG ELECTRONICS CO.,

## ABSTRACT

To improve the efficiency of the inverter rotary compressor we analyse the dynamic characteristics of the moving parts of the compressor and designed a new vane which has the reduced size and mass to decrease the inertia force of vane and the contact force between roller and vane.

Numerical analysis is used for calculating the temperature and the stress distribution of both the roller and the vane as well as the cylinder using the commercial FEM (Finite Element Method) program I-DEAS to confirm the reliability of the new vane.

We get some mechanial properties such as friction coefficients and Young's Moduli of vane and roller by the experiments.

To predict the wear characteristics of the vane at high rotating speed of roller we get the relationship between the wear rate of vane and rotating speed of the roller using AE (Acoustic Emission) technique from the wear tests.

List of symbols

| | |
|---|---|
| $a_v$ | Acceleration of vane |
| $C_x$ | x coordinate of contact point between vane and roller from vane tip center. |
| $C_y$ | y coordinate of contact point between vane and roller from vane tip center. |
| e | Eccentricity of roller center |
| $F_r$ | Contact force between vane and roller |
| $F_{in}$ | Inertia force of vane |
| $F_{vs}$ | Spring force of vane |
| k | Spring Constant |
| L | Depth of cylinder |
| $m_v$ | Mass of vane |
| N | Reaction force at vane |
| O | Origin of the cylinder |
| $O_R$ | Origin of the roller |
| $O_v$ | Origin of the vane tip radius |
| $P_c$ | Pressure in the compression chamber |
| $P_d$ | Pressure inside closed housing |
| $P_s$ | Pressure in the suction chamber |
| R | Reaction force at suppot |
| q | Distributed force |
| $\dot{q}$ | wear rate |
| $r_1$ | Outer radius of roller |
| $r_2$ | Inner radius of roller |

1. Senior Research Engineer
2. Engineer

$r_v$ Vane tip radius
$S_o$ Free length of spring
$t$ Vane slot length
$T$ Torque deo to friction between vane and roller
$T_c$ Temperature in the compression chamber
$T_s$ Temperature in the suction chamber
$v_o$ Maximum suction volume
$v_c$ Volume of the compression chamber
$W$ Weight
$w$ Thickness of vane
$x_v$ Displacement of vane
$\alpha$ Angle of $\overline{O_v O_R}$ and x axis
$\beta$ proportional constant
$\theta$ Rotating angle of crank shaft
$\kappa$ Polytropic coefficient
$\mu_r$ Coefficient of friction between vane and roller
$\mu_s$ Coefficient of friction between vane and slot

## Introduction

The rolling piston rotary compressors are widely used for the domestic air conditioners now. The advantages of this compressor are high efficiency, compact size, and light weight compared to the conventional compressors.

Now the rapid development of semiconductor enables to control the speed of the motor easily using the inverter contol technology. The compressor driven by the inverter motor has the variable rotating speed between 1800 rpm and 10800 rpm and their operation conditions generally more severe than the conventional rotary compressors.

In this paper we analyse the equation of motion of vane and roller of rolling piston rotary compressor whose speed is changed and perform the computer simulation of the motion of vane and roller. Next we design the new type of vane on the basis of analysis of motion and show the reliability of the vane. Experiments are undertaken to determine some mechanical properties of vane and roller and to exmine the wear between vane and roller.

## Equation of motion of vane and roller

We can see the construction of the rolling piston rotary compressor in Fig.1. The specification of the compressor is shown in Table 1 and the dimensions of the cylinder, vane and piston are shown in Table 2.

### 1.Definition of coordinate system and variables

The coordinates system and variables are defined to derived the equations of motion of vane and roller, as shown in Fig. 2. The main variables are the rotating angle $\theta$ of crankshaft from x- axis and the rotating angle of the piston.

2. Pressure in compression chamber

The volume of compression chamber can be calculated from the following equation :

$$V_c = [\pi r_B^2 - \pi r_1^2 - \{\pi r_B^2 \times \theta/(2\pi) - \pi r_1^2 (\theta+\alpha)/(2\pi) - \tfrac{1}{2} x_v e \sin\theta + \pi r_v^2 \alpha/(2\pi)\} - \tfrac{1}{2}(h_w + \pi r_v^2/2 \times \gamma/(2\pi) - w r_v \cos\gamma/2] \times L \quad (1)$$

where

$$\sin\gamma = w/(2r_v)$$

The maximum volume of suction chamer can be given bythe equation as follows:

$$V_o = (\pi r_B^2 - \pi r_1^2) \times L \quad (2)$$

The pressur of the compression chmber is calculated from the following equation:

$$P_c = P_s \times (V_o / V_c)^{\kappa} \quad (3)$$

The temperature of the compresssion chamber is calculated from the equation as follows:

$$T_c = T_s \times (P_c / P_s)^{(\kappa-1)/\kappa} \quad (4)$$

3.Equation of motion of vane

The forces acting on the vane are the spring force, inertia force of vane itself and contact force. The spring force $F_{vs}$ is calculated form the following equation :

$$F_{vs} = k (S_b + x_v + H_{vs} - S_o) \quad (5)$$

The inertia force $F_{vi}$ is given by the following form :

$$F_{vi} = -m w^2 g''(\theta) \quad (6)$$

where

$$g''(\theta) = -\tfrac{1}{4}[(r_1 + r_v)^2 - e^2\sin^2\theta]^{-3/2} e^4 \sin^2 2\theta + [(r_1 + r_v)^2 - e^2\sin^2\theta]^{-1/2} e(2\sin^2\theta - 1) - e\cos\theta$$

$$= \frac{\ddot{x}_v}{w}$$

The contact force $F_r$ between vane and roller is calculated from the following equation:

$$F_r = (m_v a_v - A9)/A8$$

$$= \frac{m_v a_v - \{\mu_s[2(A2 + m_v a_v w/2)/A7 - A1] + A3\}}{A6 + 2\mu_s A5/A7 - \mu_s A4} \quad (7)$$

where

$$ph = h - d - C_x$$

$$A1 = (P_s - P_c)ph \times l$$

$$A2 = F_{vs}(w/2) + P_d \times wl(w/2) + (P_c - P_s)ph^2 \times 1/2 - P_c(w/2 - C_y)l(3w/4 + C_y/2) - P_s(w/2 + C_y)l(w/2 + C_y)/2$$

$$A3 = P_c(w/2 - C_y)l + P_s(w/2 + C_y)l - F_{vs} - P_d \times wl$$

$$A4 = \sin\alpha - \mu_r\cos\alpha$$

$$A5 = \mu_r\cos\alpha \times ph - \mu_r\sin\alpha \times (w/2+C_y) - \cos\alpha \times (w/2+C_y) - \sin\alpha \times ph$$

$$A6 = \cos\alpha + \mu_r\sin\alpha$$

$$A7 = \tau + \mu_s w$$

$$A8 = A6 + 2\mu_s A5/A7 - \mu_s A4$$

$$A9 = \mu_s[2(A2 + m_v a_v w/2)/A7 - A1] + A3$$

All the forces acting on the vane are shown in Fig.3.

4. Computer simulation

We can see the results of calculation of the pressure and temperature in the compression chamber from (1) and (2) in Fig.4 - 5.

The variation of inertia force of the vane with rotating angle is shown in Fig.6 - 7. The inertia force of the of the thinner vane is reduced by 25 %.

We can see the variation of the contact force in Fig. 8 - 11. The contact force is increased by the inertia force which acts in the direction of the center of roller for the rotating angle between 90 degrees and 270 degrees. For the rotating speed of 3600 rpm, there is no effect of the inertia force on the contact force. The contact force is affected by the inertia force for the rotating speed of 7200 rpm.

By reducing the thickness of the vane, the effect of force by the back pressure is greatly reduced, as shown in Fig. 10. The effect of the reduced mass of the vane is slight,as shown in Fig. 11.

## Numerical analysis

FEM (Finite Element Method) is used to obtain the temperature, stress and deformation distribution of the vane and roller using the commercial FEM program I - DEAS. We have reduced the thickness of the vane and review the strength of the new vane and the interference of it with the slot.

We use 8 - nodes shell element in calaculation and the number of elements and nodes in use are 1176 and 1350, respectively.

The analysis is performed when the rotating angle is zero degree and 235 degree.

We can see the results of the numerical analysis in Fig. 12 - 16.

The maximum displcement of the modified vane is lager than conventional one by 5.3 % and vane tip displacement by 2.0 %. Vane tip stress of the modified vane decreases by 6.0 %. The effective stress is much smaller than the yield strength of vane material.

## Experiment

1.Measurement of friction coefficient of vane and roller

We can see the testing apparatus for coefficient of friction in Fig.17. It is calculated from the following equation :

$$\mu = \frac{T}{Nr_1} = \frac{Ta}{[Wb+(q/2)((d^2-c^2))]r_1} \quad (8)$$

The resluts of the test can be seen in Table 3.

2.Measurements of Young's Moduli of vane and roller

We measure the Young's Moduli of vane and roller by the normal mode analysis because the specimens are so small the we can not use the UTM(Universal Testing Machine) for tension or bending test. To measure the natural frequency of the specimen we use the testing apparatus shown in Fig.18.

The Young's Modulus is calculated by FEM using trial error method.The resluts of the test can be seen in Table 4.

3. Wear test

To predict the wear phenomenon between roller and vane we derive the equation using the acoustic emission technology.

In the steady state of wear process, AE energy rate is linearly proportional to wear rate . The relationship can be written in the following form :

$$\dot{E}_{AE} = \beta \mu_r N \dot{q} \quad (9)$$

To prove the equation above we performe the wear test. The chemical composition and hardness of the vane and roller are shown in Table 4.

We can see the configuration of the specimen in Fig. 19.

Block diagram of apparatus fot the wear test is shown in Fig. 20.The rotating speed is continuous duing the steady state. For the 5 different rotating speeds (118,233, 355, 455, 585 rpm ) wear test is performed.

In Fig. 21 the change of AE RMS voltage, AE peak amplitude, and AE energy rate are shown. The AE peak amplitude is increased as the rotating speed is increased. The wear rate and wear amount per running distance for various velocity is shown in Fig. 22. The wear rate in 118 and 585 rpm is smaller than that in 233 , 355 and 455 rpm. The time need to reach the steady state grows shoter as the rotating speed grows larger, shown in Fig. 23. We can see the results of the frequency analysis in Fig.24.

## Conclusion

In this research we analyze the moving parts of the rolling piston type rotary compressor for improved performance of the compressor at variable speed. The summary of the research is as following:

1. From the dynamic analysis of the vane and roller we can predict the motion of the vane and roller including forces acting on those.
2. The influence of the inertia force on the contact forceis not negligible for the rotating speed of 7200 rpm above.
3. The thickness of the vane affects the contact force for all the rotating speed.
4. The modified vane shows good reliability.
5. It is possible to predict the wear rate between vane and roller using the AE technique.

## References


1. T. Mitsunaga, et al ," Rotary compressor for 180Hz Inverter Air Conditioner ," Sanyo Tech. review, Vol.19, No. 2, pp.102 - 112, 1987.
2. User's Manual for I -DEAS Level 6, SDRC,1991.
3. E.Rabinowitz, Friction and Wear of Materials, John Wiley and Sons,Inc., 1965.
4. S. Lingard, et al ," An Investigation of Acoustic Emission in Sliding Friction and Wear Materials," Wear, Vol.130, pp.367 - 379, 1989.
5. P. Blau, Friction and Wear Transaction of Material, Noyes Publications, 1989.


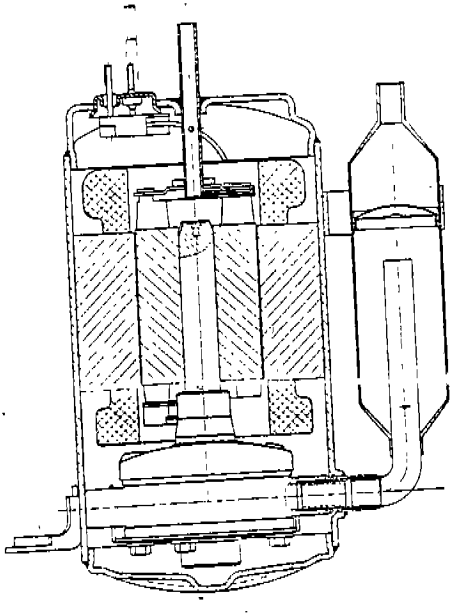

Fig. 1. A sectional view of the rotary compressor.

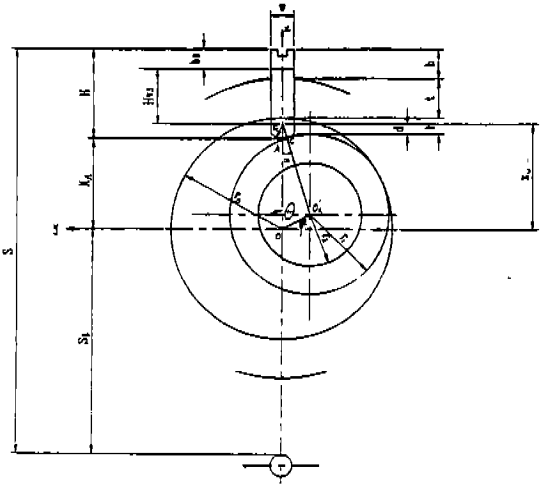

Fig. 2. Definition of coordinates and variables.

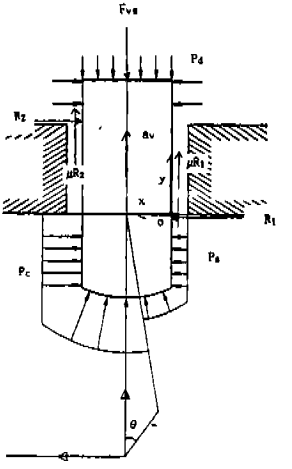

Fig. 3. All the forces acting on the vane.

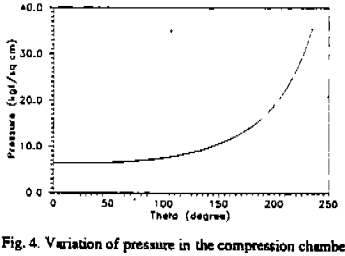


Fig. 4. Variation of pressure in the compression chamber.

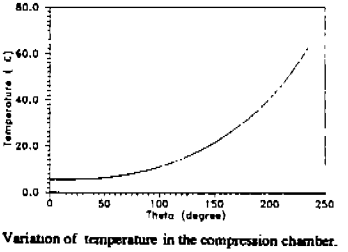


Fig. 5 Variation of temperature in the compression chamber.

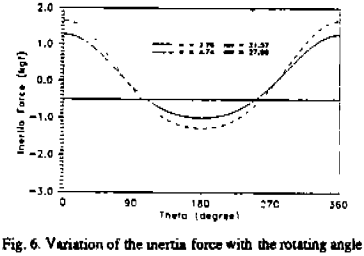


Fig. 6. Variation of the inertia force with the rotating angle (3600 rpm)

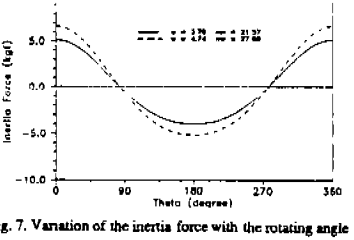


Fig. 7. Variation of the inertia force with the rotating angle (7200 rpm)

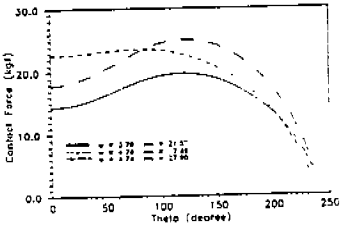


Fig. 8. Variation of the contact force with the rotating angle (3600 rpm)

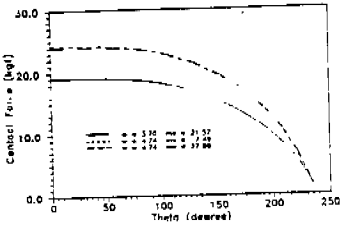


Fig. 9. Variation of the contact force with the rotating angle (7200 rpm)

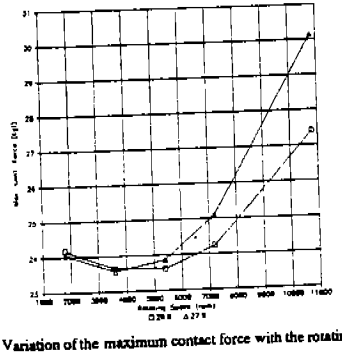

Fig. 10. Variation of the maximum contact force with the rotating speed. (mass of vane changed)

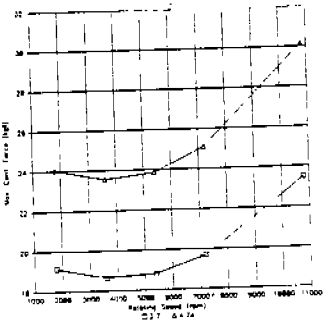

Fig. 11. Variation of the maximum contact force with the rotating speed. ( thickness of vane changed )

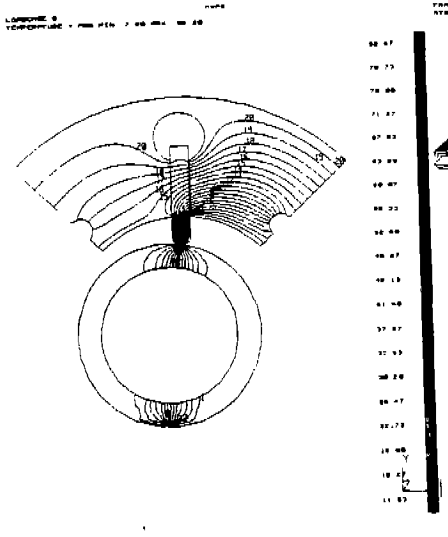

Fig. 12. Temperature field of the compressor.

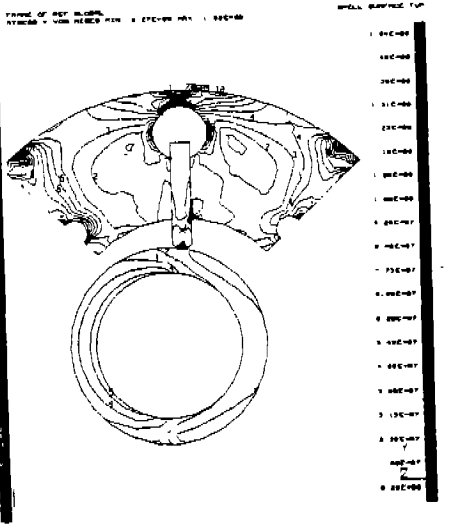

Fig. 13. Total effective stress field of the compressor.

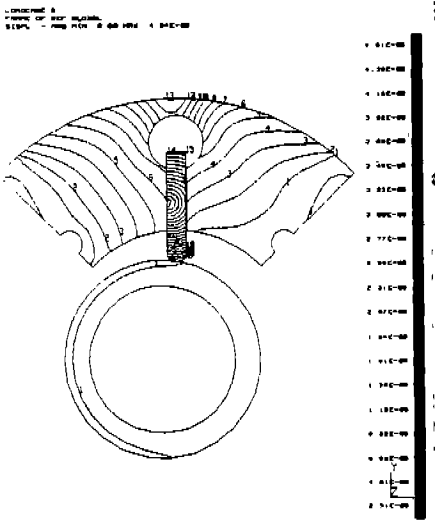

Fig. 14. Total displacement field of the compressor.

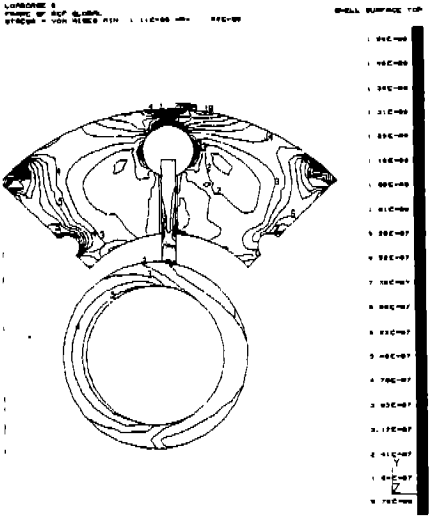

Fig. 15. Total effective stress field of the compressor ( modified vane).

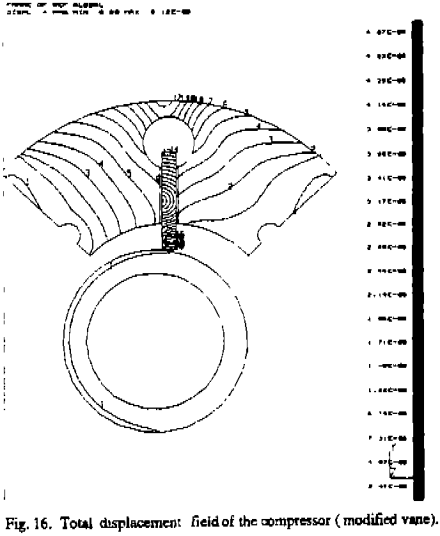

Fig. 16. Total displacement field of the compressor ( modified vane).

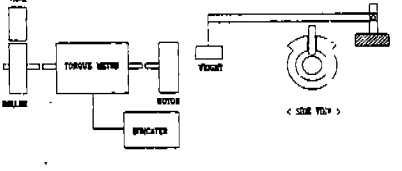


Fig. 17. Experimental apparatus for measurement of coefficient of friction.

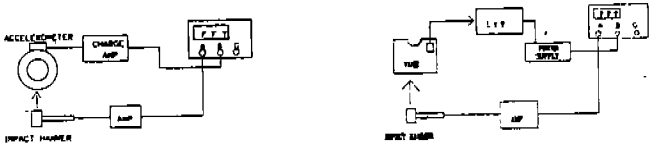


Fig. 18. Experimental apparatus for measurement of natural frequency.

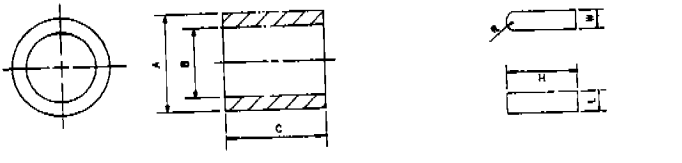


(Unit : mm)

| Specimen | A | B | C |
|---|---|---|---|
| Roller | Φ49.85 | Φ35.75 | 31.3 |

(a)

(Unit : mm)

| Specimen | L | W | H | R |
|---|---|---|---|---|
| Vane | 5.00 | 4.68 | 21.0 | 3.18 |

(b)

Fig. 19. Configuration of vane and roller. (a) roller (b) vane

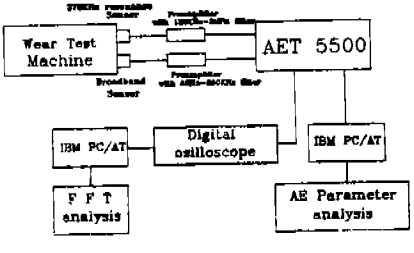


Fig. 20. Block diagram of wear testing apparatus.

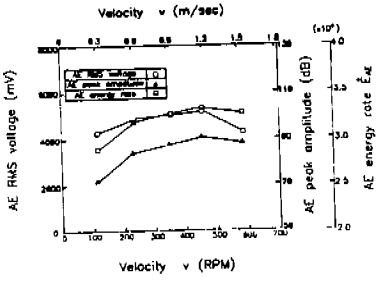


Fig. 21. AE results in wear test.

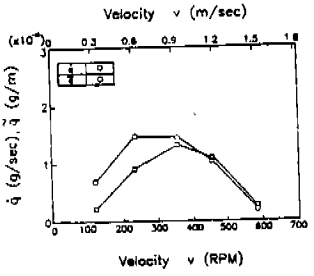


Fig. 22. Variation of wear rate with velocity.

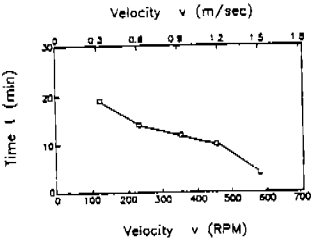


Fig. 23. Variation of time to steady state with velocity.

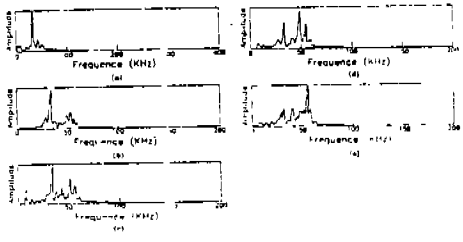


Fig. 24. Results of frequency analysis using FFT analyzer.
(a)118 rpm (b) 233 rpm (c) 355 rpm (d)455 rpm (e) 585 rpm

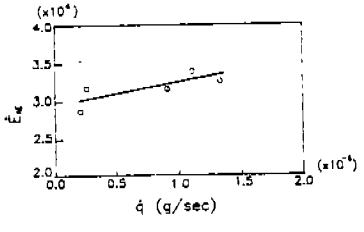


Fig. 25. Relation between AE energy rate and wear rate.

Table 1. The specification of the compressor and vane.

| | | |
|---|---|---|
| Compressor | Capacity | 11000 Btu/hr |
| | Weight | 127.5 ㎏ |
| Motor | Synchronous Speed | 3600 rpm |
| | Power | 700 W |

Table 2. The dimensions of the cylinder, vane and piston.

| | |
|---|---|
| Cylinder Diameter | 57.2 |
| Cylinder Depth | 31.3 |
| Vane Thickness | 4.74 |
| Roller Diameter | 49.9 |

Table 3. The coefficient of friction of vane and roller.

| | | |
|---|---|---|
| Wet Condition | Static | 0.103 |
| | Dynamic | 0.0588 |
| Dry Condition | Static | 0.159 |
| | Dynamic | 0.137 |

Table 4. The natural frequency and Young's modulus of vane and roller.

| | Natural Freq. (Hz) | E(GPa) |
|---|---|---|
| VANE | 24821 | 142 |
| ROLLER | 12085 | 123.5 |

Table 5. The chemical composition and hardness of vane and roller

| Specimen | Components of material (%) | | | | | | | | | | Hardness, Rc |
|---|---|---|---|---|---|---|---|---|---|---|---|
| Vane | Fe | 78.07 | W | 8.72 | Nb | 6.67 | Cr | 4.46 | V | 2.09 | 61 - 62.5 |
| Roller | Fe | 95.94 | Si | 2.58 | Cu | 0.90 | Cr | 0.71 | | | 46 - 54 |